A Fault Detection Method for Photovoltaic Systems Based on Voltage and Current Observation and Evaluation

Tingting Pei and Xiaohong Hao *

College of Electrical and Information Engineering, Key Laboratory of Gansu Advanced Control for Industrial Processes, National Demonstration Center for Experimental Electrical and Control Engineering Education, Lanzhou University of Technology, Lanzhou 730050, China; peitt52@126.com

* Correspondence: haoxh@lut.cn; Tel.: +86-093-129-735-06

check for updates

Abstract: Photovoltaic (PV) power generation systems work chronically in various climatic outdoor conditions, therefore, faults may occur within the PV arrays in PV systems. Online fault detection for the PV arrays are important to improve the system's reliability, safety and efficiency. In view of this, a fault-detection method based on voltage and current observation and evaluation is presented in this paper to detect common PV array faults, such as open-circuit, short-circuit, degradation and shading faults. In order to develop this detection method, fault characteristic quantities (e.g., the open-circuit voltage, short-circuit current, voltage and current at the maximum power point (MPP) of the PV array) are identified first to define the voltage and current indicators; then, the fault-detection thresholds are defined by utilizing voltage and current indicators according to the characteristic information of various faults; finally, voltage and current indicators evaluated at real-time voltage and current data are compared with the corresponding thresholds to detect potential faults and fault types. The performances of the proposed method are simulated verifying by setting eight different fault patterns in the PV array. Simulation experimental results show the effectiveness of the proposed method, especially the capacities of distinguishing the degradation faults, partial shading faults and variable shading faults.

Keywords: photovoltaic (PV) arrays; fault detection; voltage indicators; current indicators; partial shading

1. Introduction

With the increasing environmental concerns, solar energy has been widely used because of its inexhaustible and environmentally friendly advantages [1]. Under complex and changeable climate conditions, operational faults in a photovoltaic (PV) system have always been one of the important factors affecting its power-generation efficiency [2,3]. However, faults in the direct current (DC) side of a PV system, such as open-circuit, short-circuit, degradation and shading faults, are often difficult to avoid and can result in system energy loss, PV module lifespan reduction, or even serious safety concerns. Hence, the development of a fault detection method for the PV array faults is particularly significant for improving the energy conversion efficiency of the PV system, increasing the service life of the PV modules, and reducing maintenance cost [4,5].

Existing fault-detection methods include those based on thermal infrared detection, time domain reflectometry, artificial intelligence algorithm, mathematical model analysis methods, and so on. The thermal infrared detection method detects and identifies faults by an infrared scanner to measure the surface temperature of the PV modules for abnormal heat caused by faults. Nian et al. [6] utilizes

the principles of the semiconductor's electroluminescence to design image acquisition devices that can obtain infrared image of PV modules. The devices can detect the faults including black pieces, fragmentation, broken grid and crack for the PV modules. Peizhen and Shicheng [7] propose a method that can automatically analyze and recognize the working status of the PV arrays based on infrared image analysis. The method can accurately identify the normal, shading and degradation status of the PV modules. However, the thermal infrared detection method mainly focuses on the detection of hot spot faults inside a PV array.

The time domain reflectometry method needs to inject a pulse signal into the series PV modules circuits of a PV array, and then identifies the fault status of the PV array by comparing the input pulse signal with the feedback output signal. Takashima et al. [8,9] applies the time domain reflectometry method to detect degradation faults and locate fault positions of the PV module in a PV array by the change of response waveform. However, when utilizing the time domain reflectometry method to detect faults, the PV system must be turned off, which will critically affect the system's productivity.

In recent years, artificial intelligence algorithms have attracted the attention of scholars. The artificial intelligence algorithms include mainly artificial neural network and machine learning methods to detect PV array faults. Chine et al. [10] and Mekki et al. [11] use an artificial neural network method to detect short circuit faults and partial shading faults of a PV array. Dhimish et al. [12,13] introduce a method to distinguish short circuit faults and partial shading faults of a PV array based on fuzzy logic. Dhimish et al. [14] propose a statistical method to detect and locate accurately different faults types including a PV module fault, the PV strings faults, and a faulty maximum power point tracker (MPPT) unit. Harrou et al. [15] present a statistical monitoring approach to discriminate short-circuit, open-circuit and shading faults of a PV array. However, these algorithms need to consume longer computation time and larger memory size in the process of fault detection.

The mathematical model analysis method compares actually measuring output values with analytically computing output values to detect the fault status of a PV array. There are some mathematical modeling approaches for fault detection. For instance, references [16–18] use the one-diode model approaches to detect faults for a PV array. Kang et al. [19] propose a novel method to diagnose output power lowering in a PV array based on using the Kalman-filter algorithm. But the effectiveness of these mathematical model-based fault detection methods depends heavily on the accuracy of the models. Silvestre et al. [20] and Yahyaoui and Segatto [21] present a new procedure for automatic fault detection in grid-connected PV systems based on the evaluation of current and voltage indicators where the computational complexity is reduced through minimizing the number of monitoring sensors. However, this method cannot distinguish between degradation faults and partial shading faults of the PV modules in a PV array.

In the literature, in order to detect the potential faults and fault types of the PV array under various climate conditions, a fault-detection method based on voltage and current observation and evaluation is proposed. This method can not only distinguish the open-circuit, short-circuit, degradation and shading faults in the potential faults of the PV array, but can also recognize the variable shading faults in some special situation. Furthermore, the computational procedures of the adopted strategy have been reduced and the number of monitoring sensors have been minimized. Simulink work has been carried out to show the effectiveness of the proposed method.

The paper is structured as follows. Section 2 introduces the modeling of the PV module. In Section 3, a PV array configuration and its fault characteristics analysis are described. Section 4 completes the design of the fault-detection approach for the PV array in a PV system. The implementation of the fault detection in the PV array is provided with Section 5. Simulation results are explained in Section 6. Finally, Section 7 draws conclusions from the paper and suggests future research directions.

2. Photovoltaic (PV) Module Modeling

Numerous models of a solar cell that predict energy production have been reported in the literature. The single diode model of a solar cell is the most common model used to simulate energy

production [22]. This model is based on simulating the solar cell as a photo-generated current source connected in parallel with a diode. Taking into account the resistance characteristics and loss of solar cell materials, the serial internal resistance of the solar cell consists of recombination of carriers in the junction region of the PN junction, material resistance and contact resistance, and the parallel internal resistance of the solar cell consists of the leakage current at the edge. The equivalent circuit of the single diode model of the solar cell is shown in Figure 1.
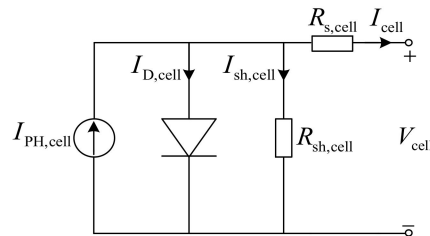
Figure 1. Single diode model of the solar cell.

The equation that mathematically describes the current and voltage characteristic of the solar cell is given by [23]:

$$I_{\text{cell}} = I_{\text{PH,cell}} - I_{0,\text{cell}}[\exp(\frac{q(V_{\text{cell}} + R_{\text{s,cell}}I_{\text{cell}})}{akT}) - 1] - \frac{V_{\text{cell}} + R_{\text{s,cell}}I_{\text{cell}}}{R_{\text{sh,cell}}} \qquad (1)$$

where I_{cell} and V_{cell} are the output current and voltage of the solar cell, respectively; $I_{\text{PH,cell}}$ is the photocurrent of the solar cell; $I_{0,\text{cell}}$ is the reverse saturation current of the diode; a is the diode's ideality factor; T is the cell's temperature; q is the electron charge ($q = 1.602 \times 10^{-19}$C); k is the Boltzmann constant ($k = 1.381 \times 10^{-23} J/K$);$R_{\text{s,cell}}$ and $R_{\text{sh,cell}}$ are the series and parallel internal resistance, respectively.

However, a PV module is generally composed of solar cells connected by series connection. According to Equation (1), the current and voltage characteristic of a PV module can be given as [23]:

$$I = I_{\text{PH}} - I_0[\exp(\frac{V + R_{\text{s}}I}{a\text{V}_{\text{t}}}) - 1] - \frac{V + R_{\text{s}}I}{R_{\text{sh}}} \qquad (2)$$

where I and V are the output current and voltage of the PV module, $I = I_{\text{cell}}$ and $V = N_{\text{cell}}V_{\text{cell}}$;$N_{\text{cell}}$ are the series connection number of solar cells; I_{PH} is the photocurrent of the PV module, $I_{\text{PH}} = I_{\text{PH,cell}}$; I_0 is the reverse saturation current of the diode, $I_0 = I_{0,\text{cell}}$; V_{t} is the thermal voltage, $\text{V}_{\text{t}} = N_{\text{cell}}kT/q$; R_{s} and R_{sh} are series and parallel equivalent resistance, $R_{\text{s}} = N_{\text{cell}}R_{\text{s,cell}}$ and $R_{\text{sh}} = N_{\text{cell}}R_{\text{sh,cell}}$.

3. PV Array Configuration and Its Fault Characteristics Analysis

In order to reduce hot spot effect effectively, the PV module is composed of solar cells connected by series and a bypass diode connected by parallel under the condition of partial shading [24]. In this paper, the improved PV modules are connected by series to constitute a PV string, then all the similar PV strings are connected in parallel to form a PV array. The simple configuration structure of the PV array comprised by two parallel connection PV strings is shown in Figure 2. In Figure 2, the main function of the series diode (named as blocking diode) in each PV string is to prevent reverse current flowing in the PV string.
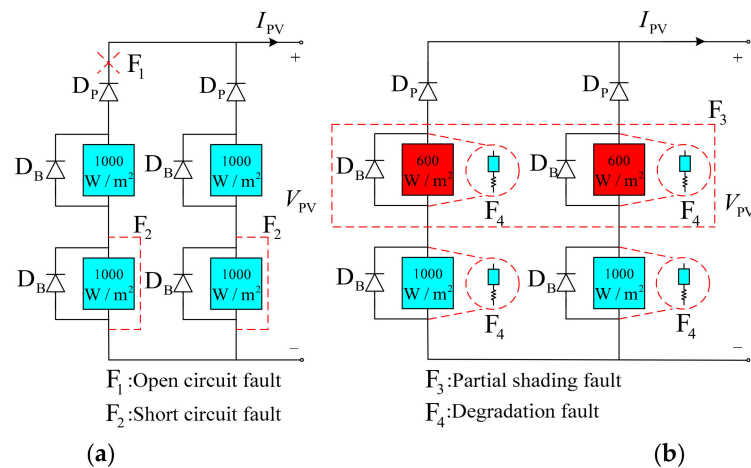
Figure 2. The configuration structure of the photovoltaic (PV) array under common fault conditions
(**a**) open-circuit and short-circuit fault; (**b**) partial shading and degradation fault.

Four well-known faults that have occurred in the DC side of PV systems (short circuit, open circuit, partial shading and degradation faults) are studied in reference [25] and [26]. An open-circuit fault may occur due to a break in wires between the solar cells by series. An open-circuit fault is shown at point 'F1' of the PV array in Figure 2a. A short-circuit fault is mainly due to bad wiring in a PV string or between PV strings. Additionally, aging, vibration and abrasion of PV modules are also the significant sources of short-circuit faults. 'F2' represents the short-circuit fault of the PV array in Figure 2a. Partial shading is the phenomenon that a PV array receives uneven irradiation and temperature caused by passing clouds, adjacent buildings and towering trees and so on [27,28]. A shading fault occurs when the part of the PV array is shaded while the other part is normally exposed to the solar irradiance with resulting output power reduction. A shading fault is indicated at point 'F3' in the PV array in Figure 2b. A degradation fault appears attributed to the failure of the bond between different layers of the module leading to delamination, some tiny cracks on the solar cell and frequent changes in temperature of the module with increasing internal series resistance. 'F4' stands for the degradation fault in the PV array in Figure 2b.

When different faults emerge in a PV array, the corresponding output characteristics of the PV array are entirely different. The output characteristic curves of the PV array under fault types set in Figure 2 are shown as Figure 3. As shown in Figure 3, when an open circuit fault occurs, the short-circuit current of the PV array decreases significantly; when a short circuit fault appears, the open-circuit voltage of the PV array reduces rapidly; when the PV array is partially shaded, the MPP current of the PV array declines obviously, but the short-circuit current and the open-circuit voltage of the PV array are basically invariant; when a degradation fault emerges, the MPP current and voltage of the PV array are reduced compared with the PV array fault-free status, and it is worth noting that the short-circuit current and the open-circuit voltage of the PV array remain unchanged. According to the above analysis, the output variables of the voltage and current at the MPP, the short-circuit current and the open-circuit voltage of the PV array happen corresponding to changes under different fault conditions. Hence, in order to achieve PV array fault detection, the voltage and current at the MPP, the short-circuit current and the open-circuit voltage of the PV array are selected as fault characteristic quantities in the paper.
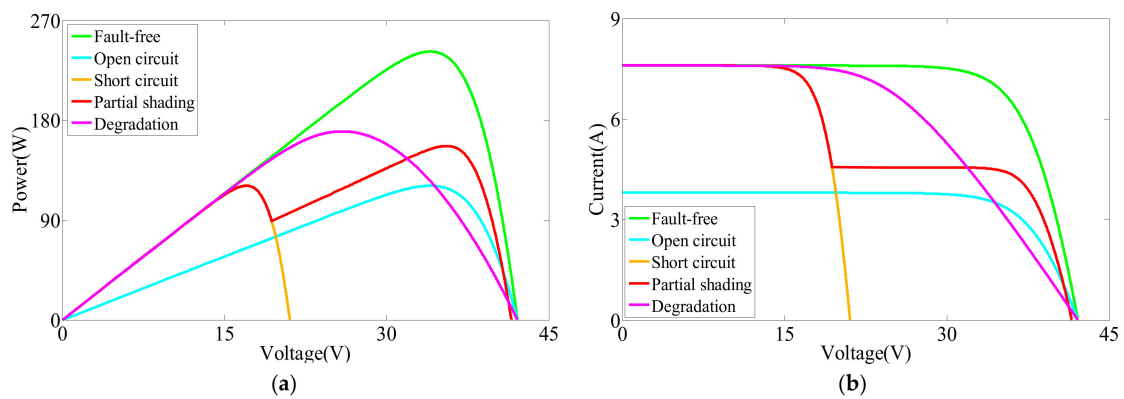
Figure 3. The output characteristic curves of the PV array under common fault conditions (**a**) power-voltage curves; (**b**) current-voltage curves.

4. Fault Detection Approach

4.1. Definition Voltage and Current Indicators

In this research, the faults relating open circuit, short circuit, partial shading and degradation of the PV array in a PV system are detected. Firstly, utilizing fault characteristic quantities, the voltage and current indicators of the PV system can be defined as follows [20]:

$$R_V = \frac{V}{V_{oc}} \tag{3}$$

$$R_I = \frac{I}{I_{sc}} \tag{4}$$

where R_V, R_I are the voltage and current indicators of the PV system, respectively; V, I are the output voltage and current at the MPP of the PV array, respectively; V_{oc}, I_{sc} are the open-circuit voltage and the short-circuit current of the PV array, and are separately given as follows [20]:

$$I_{sc} = N_p \left(\frac{I_{scm\_STC}}{1000} G + K_I (T - T_{STC}) \right) \tag{5}$$

$$V_{oc} = N_s \left(V_{ocm\_STC} + K_V (T - T_{STC}) + V_t \ln \left(\frac{I_{sc}/N_p}{I_{scm\_STC}} \right) \right) \tag{6}$$

where N_p is the number of the PV strings of the PV array; N_s is the number of the PV modules of a PV string; I_{scm_STC} is the short-circuit current of the PV module at Standard Test Conditions (irradiation: $G_{STC} = 1000W/m^2$, temperature: $T_{STC} = 25°C$); V_{ocm_STC} is the open-circuit voltage of the PV module at standard test conditions; K_I, K_V are temperature coefficients of the short-circuit current and the open-circuit voltage, respectively; G is the PV module receiving irradiation and T is the PV module temperature; V_t is the thermal voltage of the PV module.

According to Equations (3) and (4), the voltage and current indicators of the PV system in fault-free operation can be expressed by [20]:

$$R_{VM} = \frac{V_m}{V_{oc}} \tag{7}$$

$$R_{IM} = \frac{I_m}{I_{sc}} \tag{8}$$

where R_{VM}, R_{IM} are the voltage and current indicators of the PV system in fault-free operation, respectively; V_m, I_m are the output voltage and current at the MPP of the PV array during fault-free condition, and are separately given as [20]:

$$I_m = N_p(\frac{I_{mm\_STC}}{1000}G + K_I(T - T_{STC}))$$ (9)

$$V_m = N_s(V_t \ln(1 + \frac{I_{sc} - I_m}{I_{sc}}(e^{\frac{V_{oc}}{N_s V_t}} - 1)) - \frac{I_m}{N_p}R_s)$$ (10)

where I_{mm_STC} is the current at the MPP of the PV module at Standard Test Conditions. R_s is series equivalent resistance of the PV module.

4.2. Definition Fault Detection Thresholds

4.2.1. Open-Circuit Faults

When an open circuit fault emerged in one of the PV strings, the reduced portion of the output current of the PV array is equal to the current of the faulty string. Under these circumstances, the current indicator can be calculated as follows [21]:

$$R_{IO} = \frac{(N_p - 1)}{N_p}\frac{I_m}{I_{sc}} = \alpha R_{IM}$$ (11)

where R_{IO} is the current indicator when an open circuit fault is existed in the PV array; α is given as:

$$\alpha = 1 - \frac{1}{N_p}$$ (12)

Therefore, the fault detection threshold of open circuit faults are be defined by [21]:

$$T_{IO} = \varepsilon\alpha R_{IM}$$ (13)

where ε is fault detection allowed offset coefficient, $\varepsilon = 2\%$ [20]; T_{IO} is the threshold of open circuit faults, and when one or more the PV strings provided with open circuit faults, the value of R_I(given as Equation (4)) must be below the value of T_{IO}.

4.2.2. Short-Circuit Faults

Similarly, when a short-circuited PV module occurred in one of the PV strings, the reduced portion of the output voltage of the PV array is equal to the voltage of the short-circuited PV module. Based on this situation, the voltage indicator can be calculated as follows [21]:

$$R_{VS} = \frac{(N_s - 1)}{N_s}\frac{V_m}{V_{oc}} = \beta R_{VM}$$ (14)

where R_{VS} is the voltage indicator when a short-circuited PV module is present in one of the PV strings; β is given as:

$$\beta = 1 - \frac{1}{N_s}$$ (15)

Therefore, the fault detection threshold of short-circuit faults are be defined by [21]:

$$T_{VS} = \varepsilon\beta R_{VM}$$ (16)

where T_{VS} is the threshold of short circuit faults, and when one or more the PV modules in a PV string provided with short circuit faults, the value of R_V (given as Equation (3)) must be below the value of T_{VS}.

4.2.3. Partial Shading Faults

As can be seen from Figure 3b, when the part of the PV array is shaded while the other part is entirely exposed to the solar irradiance, the output current of the PV array is drastically reduced. During partial shading, the voltage and current indicators can be calculated as follows:

$$R_{VP} = \frac{V_{mp}}{V_{oc}} \tag{17}$$

$$R_{IP} = \frac{I_{mp}}{I_{sc}} \tag{18}$$

where R_{VP},R_{IP} are the voltage and current indicators of partial shading faults, respectively; V_{mp}, I_{mp} are the output voltage and current at the MPP of the PV array during partial shading with receiving the maximum irradiation, and are separately given as:

$$I_{mp} = N_P(\frac{I_{mm\_STC}}{1000}G_p + K_I(T - T_{STC})) \tag{19}$$

$$V_{mp} = N_s(V_t \ln(1 + \frac{I_{sc} - I_{mp}}{I_{sc}}(e^{\frac{V_{oc}}{N_s V_t}} - 1)) - \frac{I_{mp}}{N_P}R_s) \tag{20}$$

where G_p is the receiving maximum irradiation of the PV modules under partial shading conditions.

Therefore, the fault detection threshold of partial shading faults are be defined by:

$$T_{IP} = \varepsilon R_{IP} \tag{21}$$

where T_{IP} is the threshold of partial shading faults, and when partial or all shaded for the PV array, the value of R_I(given as Equation (4)) must be below the value of T_{IP}.

4.2.4. Degradation Faults

The majority of degradation faults can be manifested as increasing the series equivalent resistances of the degradation PV modules of the PV array, and the severe degradation of a PV module may cause a short-circuit fault the PV sting. In this paper, we only consider the case that degradation faults lead to increasing the series resistance of the degradation PV modules. As can be seen from Figure 3, if the degradation fault been present in the PV modules of the PV array, the value of R_V (given as Equation (3)) andR_I (given as Equation (4)) are, respectively, less than the value of R_{VM} and R_{IM} under fault-free operation and are separately more than the value of the short-circuit faults threshold (T_{VS}) and the open-circuit faults threshold (T_{IO}).

5. Application of the Proposed Approach in the PV Array Fault Detection

In this research, the fault detection approach for a PV array is tested in a PV system and its control scheme is shown as Figure 4. The PV system includes a PV array, a DC/DC converter, a MPPT controller and a load (described in reference [29]). Application of the proposed method in fault detection for the PV array is implemented in the following process.
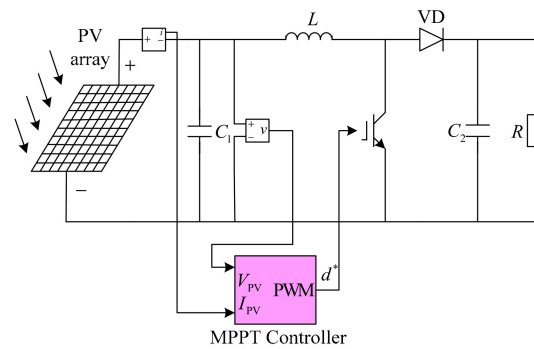
Figure 4. Control scheme for the PV system.

Step1 Initialization parameters: the number of the PV strings of the PV array (N_p); the number of the PV modules of a PV string (N_s); The PV modules receiving irradiation (G); the receiving maximum irradiation of the PV modules in partial shading conditions (G_p); the PV modules temperature (T).

Step2 Calculation of fault characteristic quantities: the open-circuit voltage and the short-circuit current of the PV array (V_{oc}, I_{sc}); the output voltage and current at the MPP of the PV array during fault-free condition (V_m, I_m); the output voltage and current at the MPP of the PV array under partial shading with receiving the maximum irradiation (V_{mp}, I_{mp}).

Step 3 Calculation of fault detection thresholds: first, evaluation the current indicator with an open fault existed in the PV array (R_{IO}), the voltage indicator with a short fault had been present in one of the PV strings (R_{VS}), the current indicator with a partial shading fault provided within the PV array (R_{IP}); Then, according to Equations (13), (16) and (21), calculation fault detection thresholds T_{VS}, T_{IO} and T_{IP}.

Step 4 Evaluation of the real-time voltage and current indicators: first, the PV system performs the MPPT strategy (proposed in [29]) and extracts the output voltage and current of the PV array (V, I); Then evaluation the real-time voltage and current indicators (R_V, R_I).

Step 5 Faults detection: according to the fault detection principles defined in Section 4.2, R_I will be respectively compared with T_{IO}, T_{IP} and R_V is compared with T_{VS} at the same time so that this goal can be achieved to detect faults and identify the types of detected faults.

Step 6 Fault alarm: if the mentioned above fault happened in the PV array, the fault alarm will be sent out. Flowchart of the proposed fault detection method is shown in Figure 5.
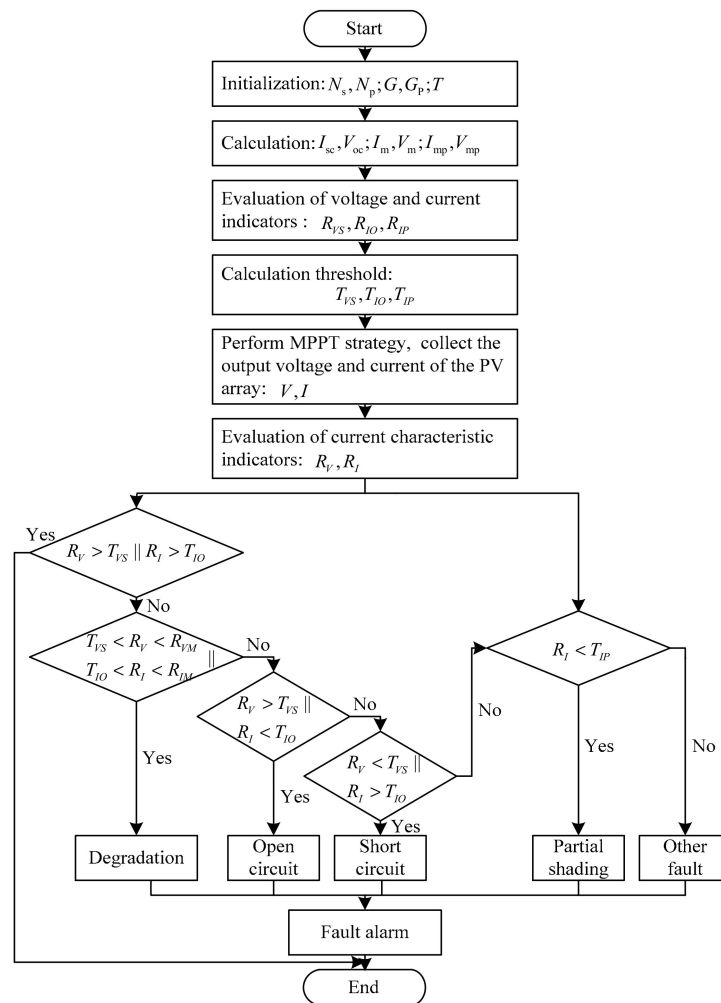
Figure 5. Flowchart of the proposed fault detection method.

6. Results and Discussion

In order to inspect the performance of the proposed method for PV array fault detection, a PV system including a fault detection unit is modelled on the MATLAB/Simulink platform. The configuration structure of the PV array is shown in Figure 6 and the key parameters of the PV modules comprising the PV array are reported in Table 1 [22]. The inputs of the fault detection unit are the real-time output voltage and current values of the PV array, and its outputs include the voltage and current indicators under fault-free conditions, the fault detection thresholds and the real-time voltage and current indicators. Then the voltage and current indicators are compared with the corresponding thresholds to detect PV array faults. The proposed scheme can not only detect the potential faults of the PV array under a test condition (receiving a certain irradiation), but identify the type of detected faults. To assess the strength of the fault detection method in the paper, eight fault types are performed in the PV array and are set as Figure 6. In the first case, the PV array shown in Figure 6 is monitored in fault-free fault. In the second case, a PV string of the PV array is opened (seen as F1 in Figure 6). In the third and fourth cases, it is assumed that the PV array contain the short-circuit faults in a PV string and between the PV strings (seen as F2 and F3 in Figure 6). In the fifth and sixth cases, degradation faults in a PV string or both two PV strings are considered (seen as F4 and F5 in Figure 6). In the seventh case, the PV array is exposed to a partial shading condition (seen as F6 in Figure 6). Under changeable climate conditions, the PV array usually experiences dynamic shading.

Hence, the performance of the proposed method is also tested and verified under variable irradiation conditions in the paper.
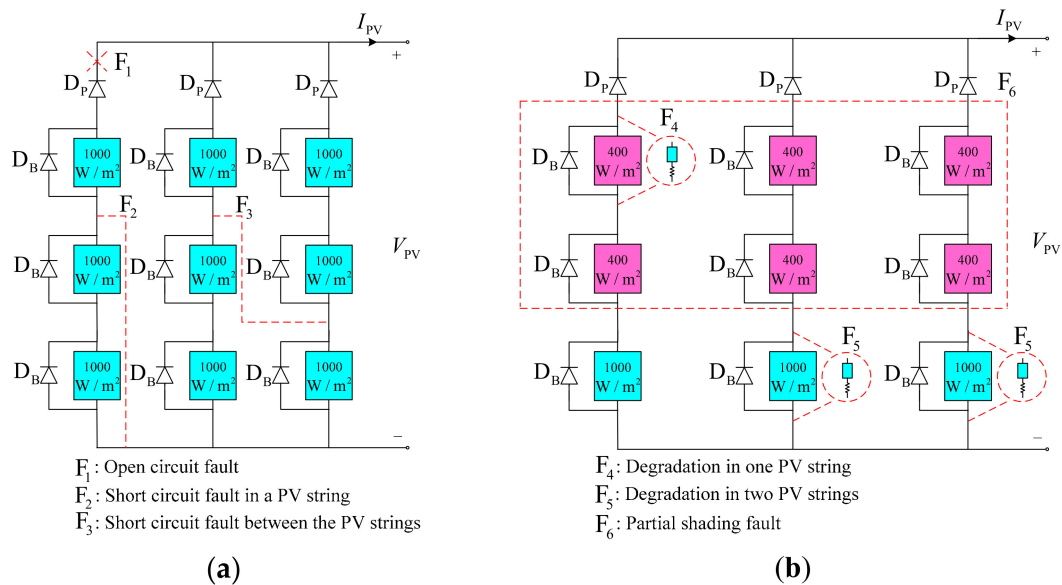

Figure 6. The configuration structure of the PV array under different fault conditions (**a**) open-circuit and short-circuit fault; (**b**) partial shading and degradation fault.

Table 1. Photovoltaic (PV) module specifications.

Parameters	Value
Maximum power	59.9 W
Voltage at open circuit	21 V
Current at short circuit	3.74 A
Voltage at the MPP (maximum power point)	17.1 V
Current at the MPP	3.5 A
Cell per module	36

6.1. Fault-Free Operation

When the PV array of the PV system described above is monitored in fault-free operation, the voltage and current indicators of the PV system are shown as Figure 7 among the PV modules temperature kept at 25°C and receiving irradiation stabilized in 1000W/m^2. Figure 7a shows the voltage indicator in fault-free operation (R_{VM}), the threshold of short circuit faults (T_{VS}) and the real-time voltage indicator of the PV system (R_V). As can be seen in Figure 7a, R_V exceeding T_{VS} indicates that the PV system is not emerged short-circuit faults. At the same time, Figure 7b shows the current indicator in fault-free operation (R_{IM}), the threshold of open circuit faults (T_{IO}), the threshold of partial shading faults (T_{IP}) and the real-time current indicator of the PV system (R_I). As illustrated in Figure 7b, R_I surpassing respectively T_{IO} and T_{IP} demonstrates that open-circuit and partial shading faults are not present in the PV system. Due to R_V and R_I several times being close to R_{VM} and R_{IM}, this means that degradation faults have not occurred in the PV system according to Section 4.2.4 and shows the effectiveness of the fault-detection algorithm under fault-free operation.
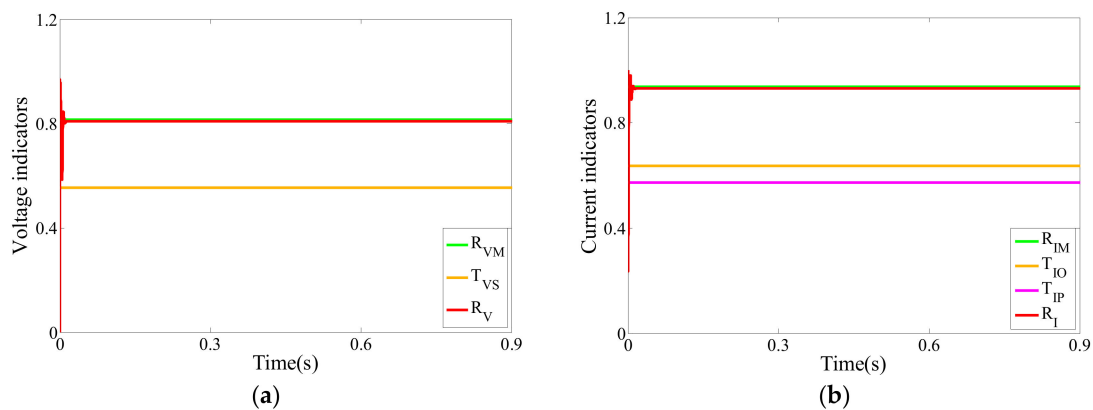
Figure 7. The voltage and current indicators of fault-free operation (**a**) voltage indicators; (**b**) current indicators.

6.2. Open-Circuit PV Strings

One of the PV strings is disconnected from the PV array, which makes the PV system provide an open circuit fault (shown as F1 in Figure 6a). Under the PV array examined at standard test conditions, the voltage and current indicators of the PV system in an open circuit fault are shown as Figure 8. On the one hand, the current indicator of R_I is below the open-circuit fault threshold given by T_{IO}, on the other hand the voltage indicator of R_V exhibits the same characteristics with fault-free operation (seen in Figure 8a,b). It is noteworthy to mention that when an open circuit fault emerged in one of the PV strings, the real-time current indicator of the PV system must be lower than the threshold of T_{IO} and the real-time voltage indicator shows the same properties with fault-free operation.
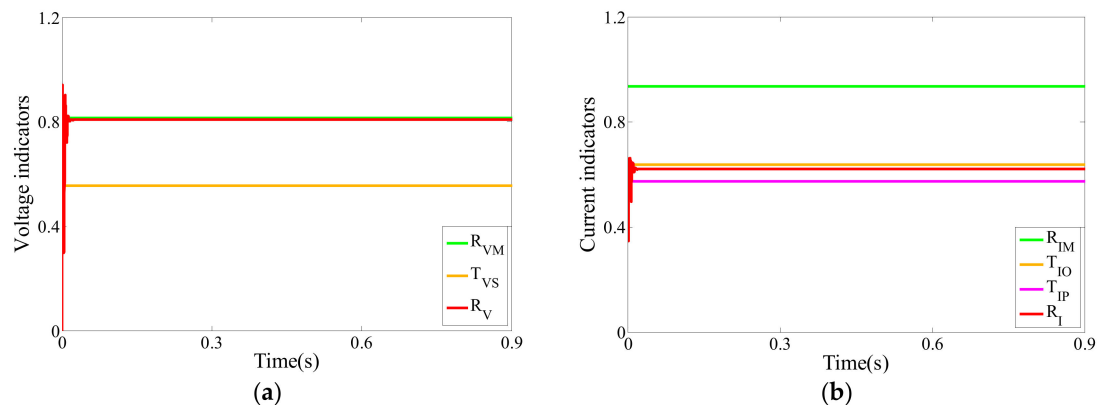
Figure 8. The voltage and current indicators of an open-circuit string of the PV array (**a**) voltage indicators; (**b**) current indicators.

6.3. Short-Circuit Faults

Two PV modules of a PV string are shorted, which makes the PV system present in short-circuit faults (shown as F2 in Figure 6a). Under the PV array examined at standard test conditions, the voltage and current indicators of short circuit faults in a PV string are shown as Figure 9. As the voltage of the short-circuited PV string decreased, the voltages of the fault-free PV strings drop to equal the voltage of the short-circuited PV string. Hence, the voltage indicator of R_V is far below the short-circuit fault threshold given by T_{VS}(seen in Figure 9a). According to the output current-voltage characteristic of the PV array, it can be seen that the output currents of the fault-free PV strings increase to equal the short current of the PV strings so that the value of R_I is slightly larger than the value of R_{IM} (seen in Figure 9b).
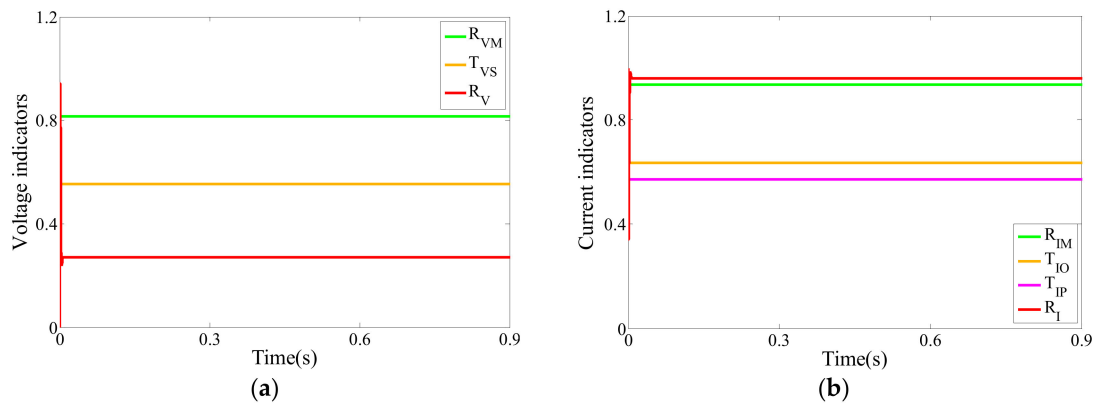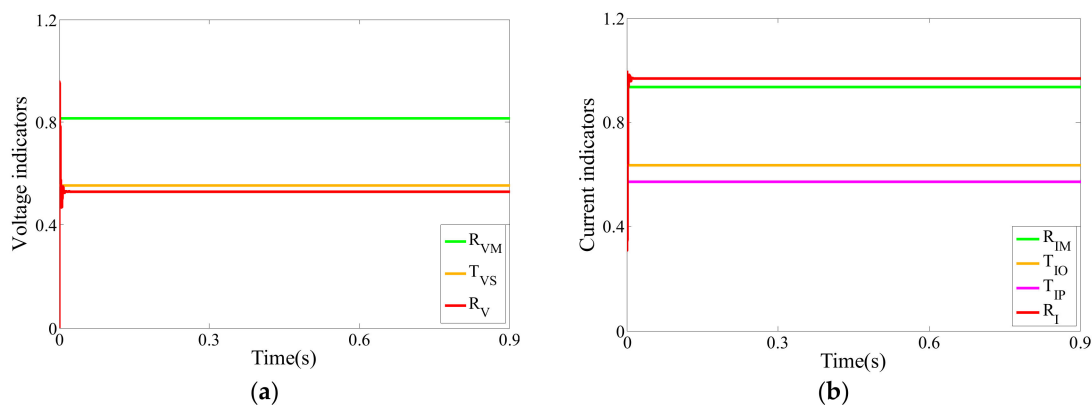
Figure 9. The voltage and current indicators of short-circuit faults in a PV string (**a**) voltage indicators; (**b**) current indicators.

The PV system experiencing a short-circuit fault between the PV strings is given as F3 in Figure 6a. The voltage and current indicators of the PV system are shown in Figure 10 at standard test conditions. The voltage indicator of R_V is below the threshold given by T_{VS} and the current indicator of R_I is slightly larger than the value of R_{IM}, which manifests a short-circuit fault been present in the PV array (seen in Figure 10a,b). The experimental result shows that the short circuit between the PV strings has less effect on the output voltage of the system than two short-circuited PV modules of a PV string.

Figure 10. The voltage and current indicators of short-circuit fault between the PV strings (**a**) voltage indicators; (**b**) current indicators.

6.4. Degradation Faults

In the PV system, a degradation fault occurring in a PV module of one of the PV strings or in two PV modules of different PV strings are separately given as F4 and F5 in Figure 6b. For this purpose, degradation faults have been simulated by inserting a resistance of 5Ω to the degradation PV modules. Under the PV array examined at standard test conditions, the real-time voltage and current indicators of the PV system in degradation faults are shown as Figures 11 and 12. The voltage indicator of R_V is more than the threshold given by T_{VS} and is evidently less than the value of R_{VM}. Similarly, the current indicator of R_I is more than the value of T_{IO} and is obviously less than the value of R_{IM}. Therefore, according to Section 4.2.4, the proposed fault detection method can commendably distinguish the degradation faults of the PV modules.
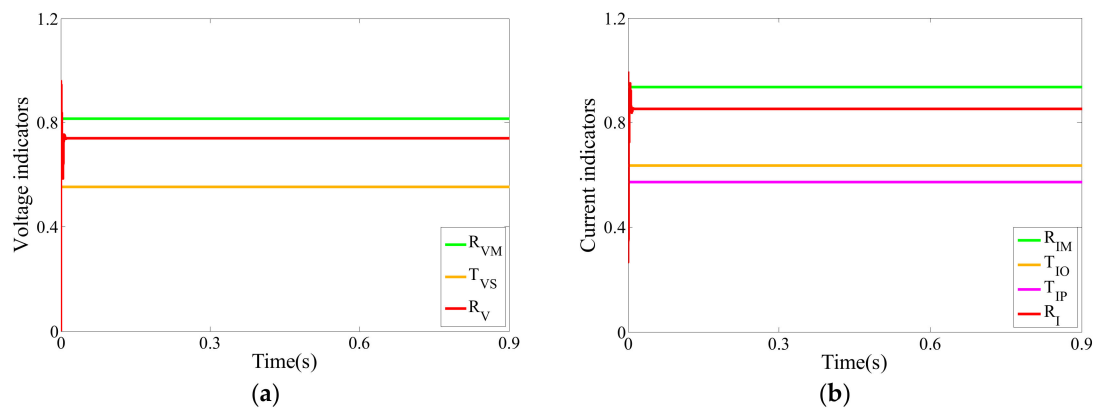
Figure 11. The voltage and current indicators of a degradation fault in a PV string (**a**) voltage indicators; (**b**) current indicators.
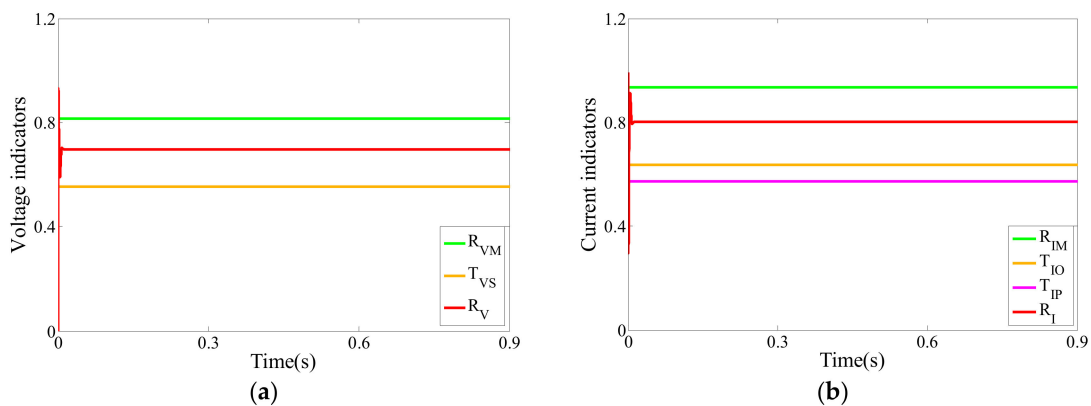

Figure 12. The voltage and current indicators of degradation faults in two PV strings (**a**) voltage indicators; (**b**) current indicators.

6.5. Partial Shading Faults

The part of the PV array is shaded while the other part is entirely exposed to irradiance with $1000W/m^2$ and the partial shading fault is set as F6 in Figure 6b. Real-time working environment data for the PV system were collected in the day with fastest weather change in the local PV power station at Gansu, China. The number of irradiation hours were 12 with the average irradiation as $690.75W/m^2$ in the day. The receiving maximum irradiation of the PV modules under partial shading conditions (G_p) is taken as $600W/m^2$ in this paper. Therefore, if a PV module receiving irradiation lower than the value of G_p, the PV module is considered to existing a partial shading fault. Under the PV array temperature kept at $25°C$, the PV array receives simultaneously two different irradiations, which are respectively $1000W/m^2$ and $400W/m^2$. In this situation, the voltage and current indicators of the PV system in partial shading faults are shown as Figure 13. The voltage indicator of R_V drops compared with the value of R_{VM}, and the current indicator of R_I is far less than the partial shading faults threshold of T_{IP}, which illustrates partial shading faults existed in the PV array.
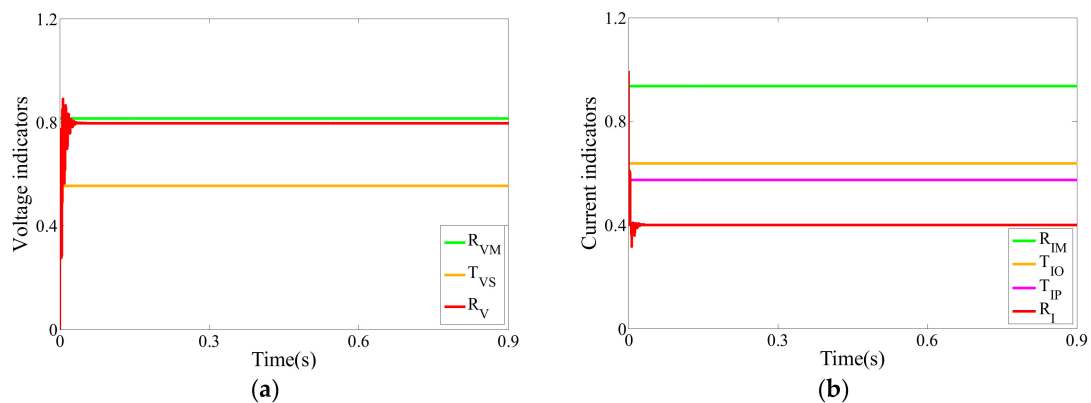
Figure 13. The voltage and current indicators of partial shading faults (**a**) voltage indicators; (**b** current indicators.

Since the PV system receiving the irradiation often changes in the actual environment, the effectiveness of the fault detection algorithm under variable irradiation conditions is validated in this paper. Under the PV array temperature kept at $25^{\circ}C$, the PV system only receives one irradiation with $1000W/m^2$ at the beginning. After 1 s, the PV modules of each PV string obtains three different irradiation, which are set as $800W/m^2$, $500W/m^2$ and $200W/m^2$ respectively. Based on this circumstance, the voltage and current indicators of the PV system in the variable shading condition are shown as Figure 14. The PV array of the PV system is considered as fault-free operation because R_V and R_I are severally close to R_{VM} and R_{IM} in 0–1 s. However, the current indicator of R_I is less than the threshold of T_{IP} and the voltage indicator of R_V drops distinctly compared with the value of R_{VM} in 1–2 s. Hence, a partial shading fault of the PV system is detected in 1–2 s. According to Figures 13 and 14, when the PV array of the PV system occurred partial shading faults, the current indicator of R_I is lower than the threshold of T_{IP}. According to Section 4.2.3, the effectiveness of the proposed method to detect partial shading faults is validated.
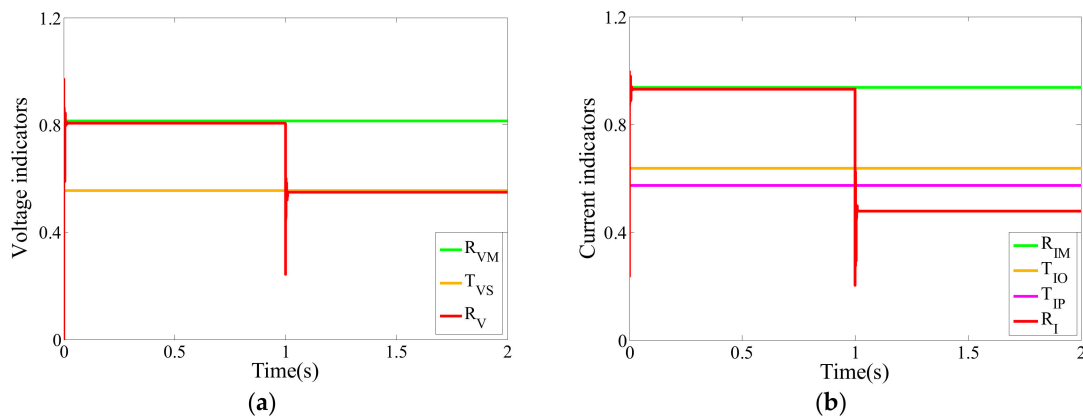

Figure 14. The voltage and current indicators of a variable shading fault (**a**) voltage indicators; (**b**) current indicators.

7. Conclusions

In the work, a fault-detection method based on voltage and current observation and evaluation has been employed to identify faults of the PV array in a PV system. This proposed method can distinguish degradation, static shading and variable shading faults under changeable climatic conditions, which is the most prominent feature of this article. Furthermore, the simple structure and low complexity of the proposed method are the key merits to implement fault detection for the PV array. The performance of the proposed method is validated based on the MATLAB/Simulink platform under all experimental

protocols (fault-free operation, an open-circuit string of the PV array, short-circuit faults in a PV string, short-circuit fault between the PV strings, a degradation fault in a PV string, degradation faults in two PV strings, partial shading and variable shading of the PV array). Results show that the proposed method can accurately detect potential faults and fault types for the PV array. Although this proposed method has successfully achieved the expected fault-detection objective, an improved fault-detection method will need to be proposed when photovoltaic arrays receive continuously changing irradiation in a certain period of time. Furthermore, in order to deal with the faults that exist in PV arrays in time, we need to further solve the problem of fault locations.

References

1. Dinçer, F. The analysis on photovoltaic electricity generation status, potential and policies of the leading countries in solar energy. *Renew. Sustain. Energy Rev.* **2011**, *15*, 713–720. [CrossRef]
2. Alam, M.K.; Khan, F.; Johnson, J.; Flicker, J. A comprehensive review of catastrophic faults in PV arrays: Types, detection, and mitigation techniques. *IEEE J. Photovolt.* **2015**, *5*, 982–997. [CrossRef]
3. Triki-Lahiani, A.; Abdelghani, A.B.B.; Slama-Belkhodja, I. Fault detection and monitoring systems for photovoltaic installations: A review. *Renew. Sustain. Energy Rev.* **2018**, *82*, 2680–2692. [CrossRef]
4. Vergura, S. Hypothesis Tests-Based Analysis for Anomaly Detection in Photovoltaic Systems in the Absence of Environmental Parameters. *Energies* **2018**, *11*, 485. [CrossRef]
5. Chen, L.; Li, S.; Wang, X. Quickest fault detection in photovoltaic systems. *IEEE Trans. Smart Grid* **2018**, *9*, 1835–1847. [CrossRef]
6. Nian, B.; Fu, Z.; Wang, L.; Cao, X. Automatic detection of defects in solar modules: Image processing in detecting. In Proceedings of the 2010 6th International Conference on Wireless Communications Networking and Mobile Computing (WiCOM), Chengdu, China, 23–25 September 2010. [CrossRef]
7. Peizhen, W.; Shicheng, Z. Fault analysis of photovoltaic array based on infrared image. *Acta Energ. Sol. Sin.* **2010**, *31*, 197–201.
8. Takashima, T.; Yamaguchi, J.; Ishida, M. Fault detection by signal response in PV module strings. In Proceedings of the IEEE Photovoltaic Specialists Conference, San Diego, CA, USA, 11–16 May 2008. [CrossRef]
9. Takashima, T.; Yamaguchi, J.; Otani, K.; Oozeki, T.; Kato, K.; Ishida, M. Experimental studies of fault location in PV module strings. *Sol. Energy Mater. Sol. Cells* **2009**, *93*, 1079–1082. [CrossRef]
10. Chine, W.; Mellit, A.; Lughi, V.; Malek, A.; Sulligoi, G.; Pavan, A.M. A novel fault diagnosis technique for photovoltaic systems based on artificial neural networks. *Renew. Energy* **2016**, *90*, 501–512. [CrossRef]
11. Mekki, H.; Mellit, A.; Salhi, H. Artificial neural network-based modelling and fault detection of partial shaded photovoltaic modules. *Simul. Model. Pract. Theory* **2016**, *67*, 1–13. [CrossRef]
12. Dhimish, M.; Holmes, V.; Mehrdadi, B.; Dales, M.; Mather, P. Photovoltaic fault detection algorithm based on theoretical curves modelling and fuzzy classification system. *Energy* **2017**, *140*, 276–290. [CrossRef]
13. Dhimish, M.; Holmes, V.; Mehrdadi, B.; Dales, M. Comparing Mamdani Sugeno fuzzy logic and RBF ANN network for PV fault detection. *Renew. Energy* **2018**, *117*, 257–274. [CrossRef]
14. Dhimish, M.; Holmes, V. Fault detection algorithm for grid-connected photovoltaic plants. *Sol. Energy* **2016**, *137*, 236–245. [CrossRef]

15. Harrou, F.; Sun, Y.; Taghezouit, B.; Saidi, A.; Hamlati, M.E. Reliable fault detection and diagnosis of photovoltaic systems based on statistical monitoring approaches. *Renew. Energy* **2018**, *116*, 22–37. [CrossRef]

16. Wang, Y.; LI, Z.; Wu, C. Four parameter on-line fault diagnosis method for PV modules. *Proc. CSEE* **2014**, *34*, 2078–2087. [CrossRef]

17. Chouder, A.; Silvestre, S. Automatic supervision and fault detection of PV systems based on power losses analysis. *Energy Convers. Manag.* **2010**, *51*, 1929–1937. [CrossRef]

18. Garoudja, E.; Kara, K.; Chouder, A.; Silvestre, S. Parameters extraction of photovoltaic module for long-term prediction using artifical bee colony optimization. In Proceedings of the 3rd International Conference on Control, Engineering & Information Technology (CEIT), Tlemcen, Algeria, 25–27 May 2015. [CrossRef]

19. Kang, B.K.; Kim, S.T.; Bae, S.H.; Park, J.W. Diagnosis of output power lowering in a PV array by using the kalman-filter algorithm. *IEEE Trans. Energy Convers.* **2012**, *27*, 885–894. [CrossRef]

20. Silvestre, S.; da Silva, M.A.; Chouder, A.; Guasch, D.; Karatepe, E. New procedure for fault detection in grid connected PV systems based on the evaluation of current and voltage indicators. *Energy Convers. Manag.* **2014**, *86*, 241–249. [CrossRef]

21. Yahyaoui, I.; Segatto, M.E. A practical technique for on-line monitoring of a photovoltaic plant connected to a single-phase grid. *Energy Convers. Manag.* **2017**, *132*, 198–206. [CrossRef]

22. Patel, H.; Agarwal, V. Matlab-based modeling to study the effects of partial shading on PV array characteristics. *IEEE Trans. Energy Convers.* **2008**, *23*, 302–310. [CrossRef]

23. Villalva, M.G.; Gazoli, J.R.; Filho, E.R. Comprehensive approach to modeling and simulation of photovoltaic arrays. *IEEE Trans. Power Electron.* **2009**, *24*, 1198–1208. [CrossRef]

24. Chunhua, W.U.; Zhou, D.; Zhihua, L.I.; Li, F.U. Hot spot detection and fuzzy optimization control method of PV module. *Proc. CSEE* **2013**, *33*, 50–61. [CrossRef]

25. Garoudja, E.; Harrou, F.; Sun, Y.; Kara, K.; Chouder, A.; Silvestre, S. Statistical fault detection in photovoltaic systems. *Sol. Energy* **2017**, *150*, 485–499. [CrossRef]

26. Mansouri, M.; Hajji, M.; Trabelsi, M.; Harkat, M.F.; Al-khazraji, A.; Livera, A.; Nounou, H.; Nounou, M. An effective statistical fault detection technique for grid connected photovoltaic systems based on an improved generalized likelihood ratio test. *Energy* **2018**, *159*, 842–856. [CrossRef]

27. Ishaque, K.; Salam, Z. A review of maximum power point tracking techniques of PV system for uniform insolation and partial shading condition. *Renew. Sustain. Energy Rev.* **2013**, *19*, 475–488. [CrossRef]

28. Li, G.; Jin, Y.; Akram, M.W.; Chen, X.; Ji, J. Application of bio-inspired algorithms in maximum power point tracking for PV systems under partial shading conditions—A review. *Renew. Sustain. Energy Rev.* **2018**, *81*, 840–873. [CrossRef]

29. Tingting, P.; Xiaohong, H.; Qun, G. A Novel Global Maximum Power Point Tracking Strategy Based on Modified Flower Pollination Algorithm for Photovoltaic Systems under Non-Uniform Irradiation and Temperature Conditions. *Energies* **2018**, *11*, 2708. [CrossRef]